LA-5548-MS
Informal Report

Experimental Observations of Underwater Detonations Near the Water Surface

los alamos
scientific laboratory
of the University of California
LOS ALAMOS, NEW MEXICO 87544

UNITED STATES
ATOMIC ENERGY COMMISSION
CONTRACT W-7405-ENG. 36

In the interest of prompt distribution, this LAMS report was not edited by the Technical Information staff.

Printed in the United States of America. Available from
National Technical Information Service
U. S. Department of Commerce
5285 Port Royal Road
Springfield, Virginia 22151
Price: Printed Copy $4.00 Microfiche $1.45

LA-5548-MS
Informal Report
UC-34
Reporting Date: February 1974
Issued: April 1974

los alamos
scientific laboratory
of the University of California
LOS ALAMOS, NEW MEXICO 87544

Experimental Observations of Underwater Detonations Near the Water Surface

by

B. G. Craig

Full support was provided by the U.S. Atomic Energy Tamarin Committee, funded by the Division of Military Application.

EXPERIMENTAL OBSERVATIONS OF UNDERWATER DETONATIONS NEAR THE WATER SURFACE

by

B. G. Craig

ABSTRACT

The results of a photographic study of the flow of water resulting from the detonation of small spheres of PBX-9404 explosive initiated at their center and submerged to various depths are given. A qualitative description of the mechanism by which a charge detonated at the upper critical depth generates a maximum amplitude water wave is proposed.

I. INTRODUCTION

A plot of wave amplitude vs depth of a given charge of explosive shows two maxima. One maximum — called the upper critical depth (UCD) — occurs when the charge is between one-half and just fully submerged. LeMehaute[1] has reviewed the theory of water waves generated by explosions at various depths in water.

The prediction of the amplitude of water waves generated by large-energy explosions has been based on extrapolation of empirical correlations between wave amplitude and charge energy of small-energy charges. The mechanism by which a spherically expanding detonation located at the UCD produces a maximum amplitude water wave has not been adequately studied. The effects near the explosion need to be understood in order to develop a model which can be used to predict water waves generated by large explosions.

Qualitatively, a spherically expanding detonation near the UCD results first in an expanding hemispherical gas bubble in the water and a mushroom cloud which becomes taller and fades with time. Very early an energetic water jet emerges from the top of the cloud. The stem of the mushroom cloud appears to be water and detonation products. A perturbation, which appears to be a mirror image of the water jet emerges from the bottom of the gas bubble. Later, the gas bubble reaches its maximum size and begins to collapse first from the bottom. The momentum of the collapsing water creates a plume. The shape, size, and collapse of the plume are apparently influenced by details of the bubble collapse, by the remnant of the water encasing the stem of the mushroom cloud, and by water falling back from the jet. In turn, these factors govern the waves generated and are governed by the depth of the charge.

Preliminary experiments and computer modeling of the phenomena near a detonation at the UCD were described in LA-4958.[2] Additional experiments are described in this report. Quantitative data which describe gas cloud size and shape, gas cavity size and shape, plume height and shape, and other data useful for developing and calibrating a model are given.

II. EXPERIMENTAL ARRANGEMENT

The experiments were performed in a tank a little larger than 7 m long by 6 m wide by 3 m deep. The tank had two water-tight windows through which the gas bubbles generated by the detonations were photographed. Each window was about 2.5 m wide by 2 m high extending about 70 mm above water level;

the window panes were 25-mm-thick Plexiglas. In some of the experiments a screen of etched Mylar film was placed behind the window farthest from the cameras and tilted to provide a uniform white background regardless of the position of the sun.

The gas bubbles were photographed with three framing, or cine, cameras: 1) a synchronous-motor-driven camera (Mitchell) operating at 64 frames/sec with color film, 2) a spring-driven camera (Bolex Model No. 16 Reflex) also operating at 64 frames/sec with black-and-white film, and 3) a variable speed camera (Hycam) operating at various speeds between 800 and 1700 frames/sec with black-and-white film.

A second synchronous-motor-driven camera was used to photograph a field which extended from about 10 m above the water level to the lower half of the nearest window. This camera also operated at 64 frames/sec with color film.

A third synchronous-motor-driven camera, operated at 28 frames/sec with black-and-white film, was located at different positions near the water level, and photographed an overall view of the experiments.

In a few experiments a sixth camera, another spring-driven Bolex operating at 64 frames/sec, was placed near one corner of the water tank for a close-up view of the detonation and resulting water motion.

The cameras were started with an automatic electronic delay system which was designed to allow all of the cameras to stabilize at their specified speeds before the detonator was fired. Unfortunately, the highest speed camera (Hycam) would not stabilize at the desired speed (ca 1000 frames/sec) with enough film left to cover all of the event. The control circuit was modified so that the Hycam camera would have full-time coverage at the expense of a stable speed.

A vertical mast with crossarms spaced 1.52 m (5 ft) center to center was located adjacent to the tank and at approximately the same distance from the camera as was the plume. This device served as a space scale for above-surface photography. A grid, 305 mm (1 ft) center to center, submerged in the tank where the charge was to be located and perpendicular to the camera axis, was photographed to provide an underwater space scale for all but the Hycam camera. The grid was removed prior to the detonation of each charge. Measurement of both front and rear windows, their images, and placement of the explosive at the midpoint between the two windows allows determination of a space scale for the Hycam camera.

The explosive charges were spheres of PBX-9404 initiated at their centers with an XTX-MDF (mild detonating fuse) spherical initiating assembly. Spheres of two diameters were used, the small sphere was 25.4 mm in diam, the larger was 50.8 mm in diam. The density of the PBX-9404 was 1.84 Mg/m^3 The MDF (usually ca 456 mm long) extended well above the water to a detonator so that the influence of the detonator was small. The explosive train was previously shown to result in a spherically expanding detonation by most of the PBX-9404. The arrival trace at the surface of the spheres is typically within 0.03 μsec except for the area within 10° of the MDF; this area was above the water surface for experiments near the UCD. Mader has shown that for practical purposes the XTX-MDF assembly within the spheres may be considered as PBX-9404.

Three methods of supporting the charge were used. In all methods the detonator cable passed through a hollow, flexible aluminum boom 25-mm square which was guyed with string and tape. In one method the detonator cable was allowed to hang down from the end of the boom and support the charge at the desired depth. This resulted in the MDF being vertical and in the tip of the boom being almost 1.5 m vertically above the main charge. In another method, a No. 50 cotton thread was glued to the PBX-9404 sphere with Eastman 910 adhesive and the thread made taut so that the detonator cable and the thread supported the charge at the desired depth but angled from the tip of the boom. A second thread was tied to the detonator so that the angle of the MDF with respect to the vertical could be controlled by adjusting the tension on the two threads. In the third method a thread was tied only to the cable above the detonator and drawn taut so the MDF was vertical but the charge was supported at a horizontal distance from the tip of the boom. In all methods the boom was adjusted as necessary to place the charge near the center of the tank.

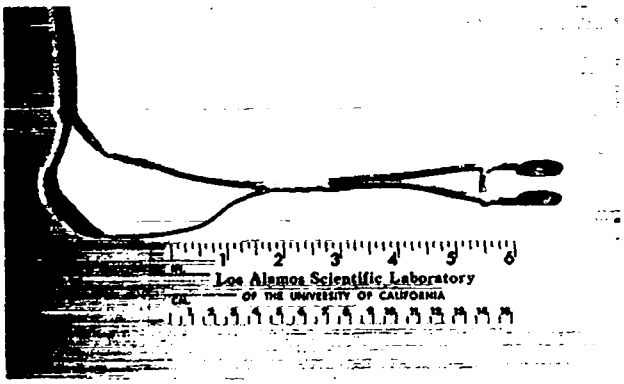

Fig. 1. Photograph of a two-penny conductivity gauge.

In all experiments a telescopic arrangement allowed an observer in the firing bunker to ascertain that the charge was at the proper depth and that the surface waves were negligible. The tank was deliberately located in a narrow box canyon protected from the wind.

In order to obtain data about subsurface flow, mass markers in the form of perforated, colored ping-pong balls were suspended in a plane near the charge axis and perpendicular to the camera axis by No. 50 cotton thread. The motions of these mass markers were recorded by the cameras which recorded the histories of the gas bubbles.

In addition, two conductivity gauges were used in the ninth and tenth experiments of this series (Shots E-3789 and E-3790). Each gauge consisted of two copper disks approximately 13 mm apart as shown in Fig. 1. The conductivity of the material within each gauge was recorded with a two-channel oscilloscope and an appropriate circuit. The gauges were located so they would be engulfed by the detonation products in the expanding bubbles at times which could be correlated with the camera photographs.

III. QUALITATIVE OBSERVATIONS

The framing camera records have been assembled as Los Alamos Scientific Laboratory (LASL) Motion Picture X-256. A study of the pictures has led to the following qualitative observations.

A spherically expanding detonation near the UCD results first in an expanding gas bubble which is approximately hemispherical in the water, a mushroom cloud which becomes taller and fades with time (indicating that the cloud is mostly detonation products), and a water jet which forms very early and goes very high. The stem of the mushroom cloud appears to be encased by water and the interior of the stem appears to be partly confined detonation products. After the mushroom cloud fades, the water encasing the stem and the jet have a combined appearance similar to that of an inverted funnel. A perturbation, termed a root, emerges from the gas bubble and flows mostly downward; the root is akin to a mirror image of the water jet. The root appears to be mostly water colored by detonation products, especially carbon.

Later, the gas bubble reaches its maximum size and begins to collapse first from the bottom. The collapse appears to become reentrant. The momentum of the collapsing water throws up a plume. The shape, size, and collapse of the plume are apparently influenced by details of bubble collapse, by the remnant of the water encasing the stem of the mushroom cloud, and by water falling back from the jet.

When the charge is significantly above UCD a smaller, or no, water jet is generated; likewise, a smaller, or no, root is formed. The resulting plume is high but narrow and appears to remain highly organized relative to plumes from charges near the UCD. The collapse of the plume is devoid of significant outward motion and forms a second hemispherical cavity in the water - also in contrast to the phenomena for charges near the UCD.

It appears that detonation only a little below the UCD produces larger water jets and roots than those at UCD. Detonations significantly below UCD (more than one charge diameter) result in gas bubbles which have their maximum diameter below the surface. In the extreme the bubble generated does not vent to the surface until it has undergone one or more oscillations. Any constriction at the surface modifies the way a plume is thrown up due to both constrictive effects and possible changes in the way the bubble collapses. Detonations below UCD which also vent significantly during expansion of the gas bubble appear to result in larger stems, the remnants of which apparently interfere with eruption of plumes. There is some indication that such detonations result in an increase in the water content of the mushroom cloud. Finally, for deep detonations there

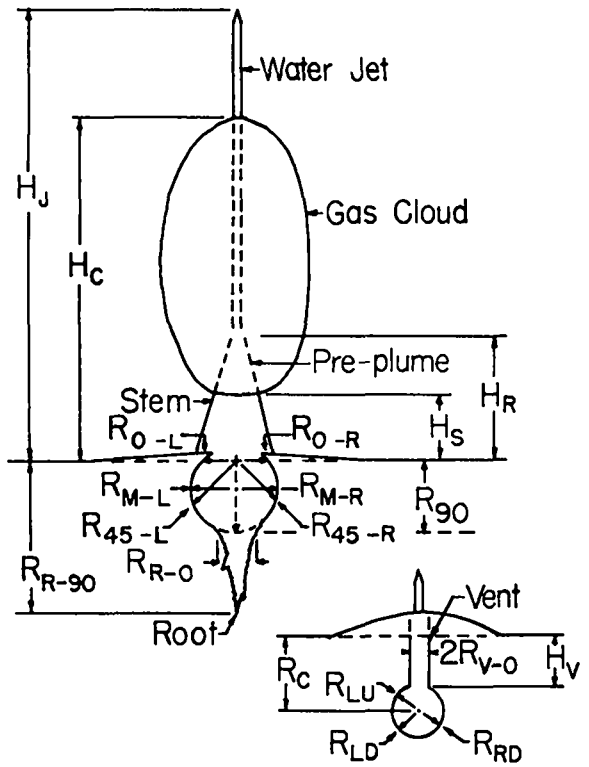

Fig. 2. Sketch with identification of most of the measurements plotted in the data section. Numbers indicate angular position in degrees from charge origin.

are neither jets, roots, nor mushroom clouds. Plume formation is the result of an entirely different mechanism.

Sketches in which the water jet, mushroom cloud and stem, gas bubble, and root are identified are given as Fig. 2.

IV. RESULTS

A summary of the shots and of selected data is given in Table I. Some of the quantitative data which can be deduced from measurements of the photographic records are plotted in Figs. 3 - 23. With only a few exceptions as noted in the captions, the data plotted are from records obtained with cameras equipped with synchronous motors. Zero time was taken as that of either the frame in which detonation light was recorded or the frame before the one in which a significant gas bubble or cloud of detonation products was recorded. Radii were measured from the intersection of a plumb line through the charge center and the original water level except as noted in the captions or in Fig. 2. Heights were measured vertically above the original water level. Plume heights are not well defined; the author recorded a height which seemed most representative to him.

The error in measurements of space below water level is estimated to be no more than 50 mm, usually about 25 mm. The error in measurements of space above water level is estimated to be no more than 150 mm, usually less than 100 mm. The greatest uncertainty in above-surface measurements is due to inability to characterize plume height because of the irregular and indeterminate shape of the plume. The maximum error in time is less than one frame time for data obtained from the synchronous-motor-driven cameras. Comparison of data recorded with both spring-driven and synchronous-motor-driven cameras is also less than one frame time (15.6 msec). As discussed under the section EXPERIMENTAL ARRANGEMENT, the Hycam camera did not operate at a constant speed. However, it is possible to find framing rates (ca 1000 frames/sec) which will make space and time measurements from the Hycam consistent with space and time measurements from the synchronous-motor-driven camera.

Figures 3 - 18 show data for 25.4-mm-diam charges. Figures 14 - 18 show the motion of the mass markers as a function of frame number (64 frames/sec). Only selected frames are plotted and identified but the solid lines are based on measurement of additional frames. Dotted lines correspond to frame times when the mass markers could not be clearly seen. The numbers near the various points are the frame numbers where frame zero corresponds to time zero (the frame with detonation light or the frame before the first recorded significant event). Some mass markers are plotted on the opposite side of vertical than their real location; also the paths of some mass markers have been omitted because either they were off scale or they were similar to paths plotted.

Figures 19 - 21 show data for 50.4-mm-diam charges. Of the two shots fired with this size charge, the largest gas bubble was generated by the charge just fully submerged. The eruption of the plume for the charge submerged 1/2 diam appeared to be through the middle of the remnant of the stem; this is in contrast to observations for shots with

TABLE I

SUMMARY OF SHOTS AND SELECTED DATA

Shot No.	Fig.	Charge diam (mm)	Charge Z (mm)	MDF Angle (° from Vertical)	Gas Bubble R-45 / R-0 (mm)	Gas Bubble t-45 / t-0 (sec)	Gas Bubble t_{co} (sec)	Jet t_b (sec)	Jet t_ℓ (sec)	Plume t_c (sec)	Plume $\frac{H_p \times D_p}{t_m}$
E-3684	3,4	25.4	+6.4	0	457 / 453	0.18 / 0.16	0.33	None	None	1.02	0.80 x 0.50 / 0.72
E-3680	5	25.4	0	0	482 / 476	0.15 / 0.15	0.39	0.45	2.95	1.31	0.80 x 1.15 / 0.73
E-3685	6	25.4	0	30	500 / 489	0.14 / 0.14	0.36	0.44	2.31	1.00	0.75 x 1.10 / 0.59
E-3689	7	25.4	-3.2	60	552 / 551	0.19 / 0.16	0.42	0.52	2.95	1.33	0.70 x 1.10 / 0.63
E-3681	8	25.4	-6.4	0	510 / 510	0.17 / 0.16	0.42	0.48	3.22	1.31	0.87 x 1.20 / 0.88
E-3686	9	25.4	-6.4	30	535 / 535	0.15 / 0.14	--	--	--	1.04	0.63 x 1.10 / 0.52
E-3690	10	25.4	-6.4	75	545 / 531	0.17 / 0.15	0.42	0.50	2.58	1.31	0.75 x 1.20 / 0.67
E-3682	11	25.4	-12.7	0	529 / 529	0.15 / 0.14	0.41	0.44	2.25	1.08	--
E-3683	12	25.4	-152.0	0	479 / 479	0.09 / 0.08	0.38	0.44	2.53	1.06	--
E-3691	13	25.4	-610.0	0	456[a]	0.05[a]	0.09[a]	None	None	1.28	1.35 x 1.00 / 0.52
					371	0.13	0.18				
					325	0.21	0.24				
					302	0.27	--				
E-3687	19	50.8	0	30	850 / 850	0.22 / 0.20	0.49	0.65	2.30	1.30	1.20 x 1.70 / 0.67
E-3692	20	50.8	-25.4	0	920 / 912	0.21 / 0.18	0.52	0.55	3.23	1.66	1.00 x 1.75 / 0.64

Key:

Charge Z = position of the center of charge listed below (-) or above (+) the water surface.

Bubble R = maximum radius measured at the angle from vertical as shown in Fig. 2. Averages of left and right measurements are tabulated.

Bubble t = time after detonation when bubble reaches maximum radius at the indicated angle.

Bubble t_{co} = time of complete collapse along vertical.

Jet t_b = time at which bottom of water jet appeared to stop moving up.

Jet t_ℓ = time at which last resolved drops from jet fell back to the surface.

Plume t_c = complete collapse time of plume.

Plume H_p = maximum height of plume in m.

Plume D_p = maximum diameter of plume in m.

Plume t_m = time in seconds when maximum height and diameter were observed.

[a] Radii and times given are the average of all four 45° measurements. The first listed is for the initial bubble, the second listed is for the second, etc., as the bubble alternately expands and collapses.

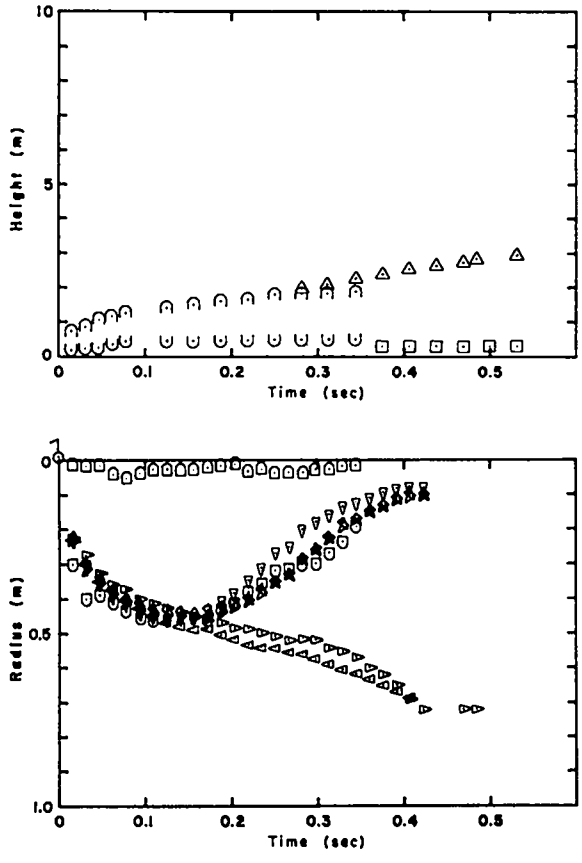

Fig. 3. Early time history (from detonation to collapse of the gas bubble) of Shot E-3684. The charge was 25.4 mm in diam, submerged 1/4 diam, supported so that the MDF was vertical and the support boom would have interfered with the water jet had there been one. In this experiment only the plume generated by the collapse of the gas bubble fell back to generate a cavity which in turn collapsed to form a second plume shown in Fig. 4.

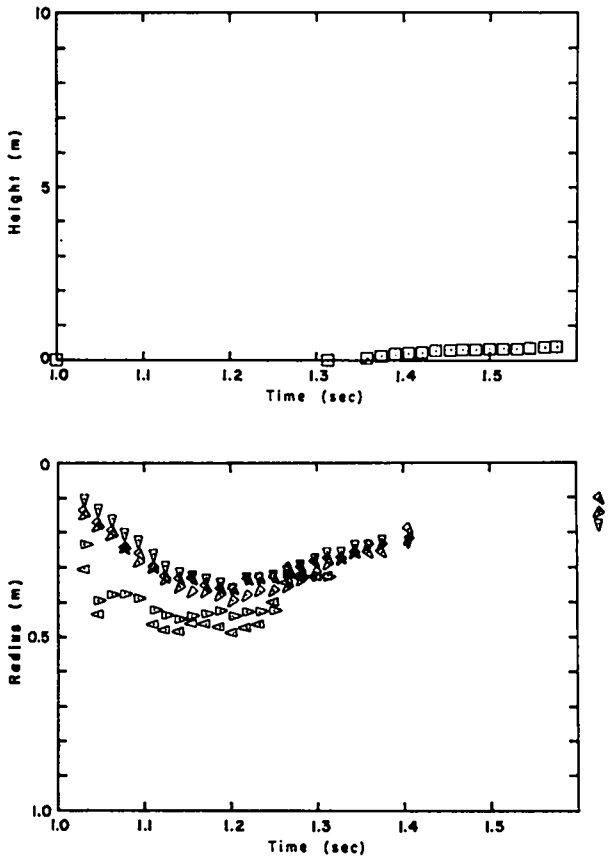

Fig. 4. Late time history of Shot E-3684. Symbols defined below.

Upper Graphs (above-surface):

- H_c, height of the top of the gas products cloud
- H_s, height of the bottom of the gas products cloud
- H_j, height of the top of the jet (in this case only, the jet was mostly gas)
- H_p, height of the plume

Lower Graphs (sub-surface):

- R_{0-L}, left side bubble radius at original water level
- R_{0-R}, right side bubble radius at original water level
- R_{45-L}, bubble radius along 45° to the left of plumb
- R_{45-R}, bubble radius along 45° to the right of plumb
- R_{90}, bubble radius along plumb
- R_{-90}, vertical length of root and bubble
- R_{R-0}, one-half of root diam near the bottom of the bubble

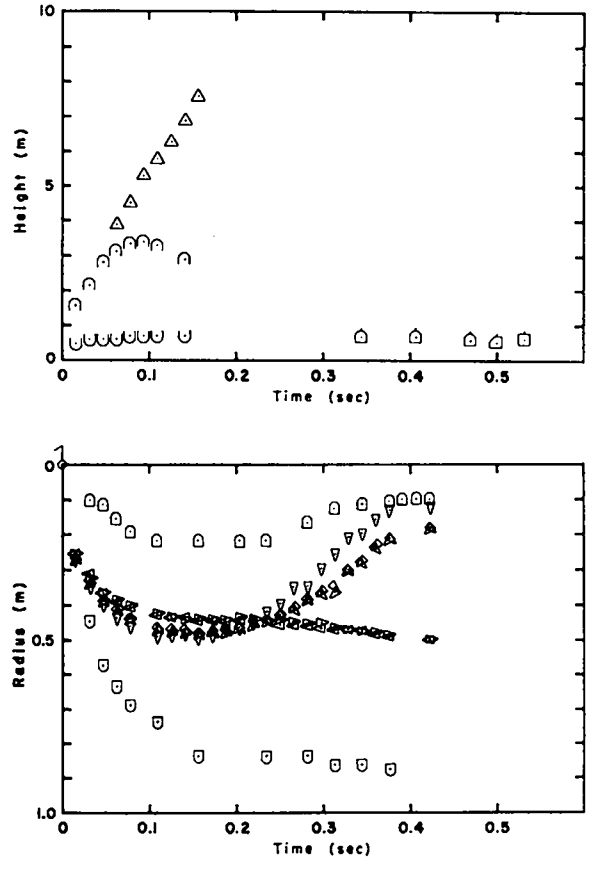

Fig. 5. Time history of Shot E-3680. The charge was 25.4 mm in diam, submerged one-half diam, and supported so that the MDF was vertical and the support boom interfered with the water jet. The symbols are defined in the caption of Fig. 3 with the addition of

$H_{R,P}$, height of remnant of stem, possibly combined with young plume

H_P , height of plume. The symbol shape is a stylized representation of the actual shape at the indicated time.

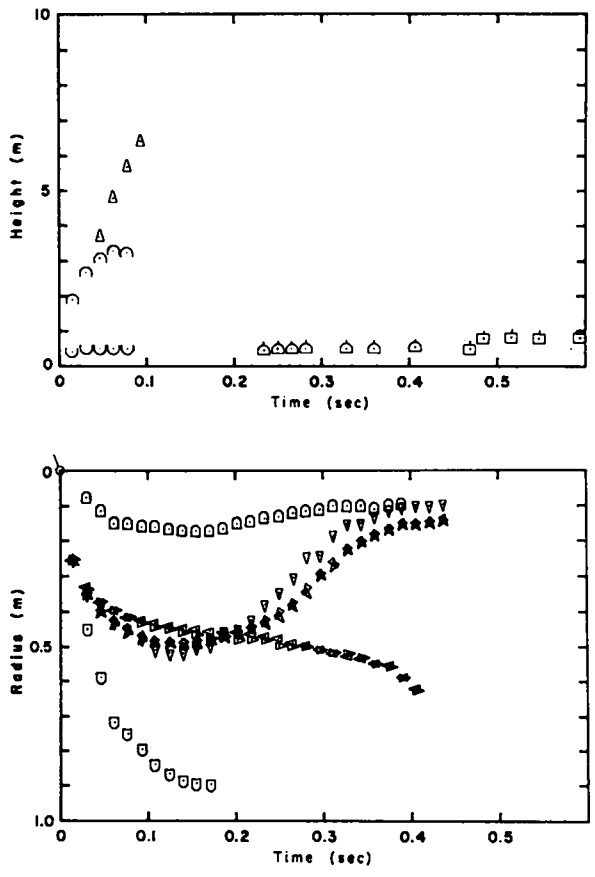

Fig. 6. Time history of Shot E-3685. The charge diameter and depth of submersion were identical to those for Shot E-3680 (Fig. 5) but the support differed. The charge was supported in part by thread so that the MDF was inclined 30° from the vertical and the support boom did not interfere. The synchronous motor camera failed to yield a record of the sub-surface for this shot so the spring-driven camera record was used to obtain the data plotted in the lower graph. The symbols are defined in the captions of Figs. 3 and 5.

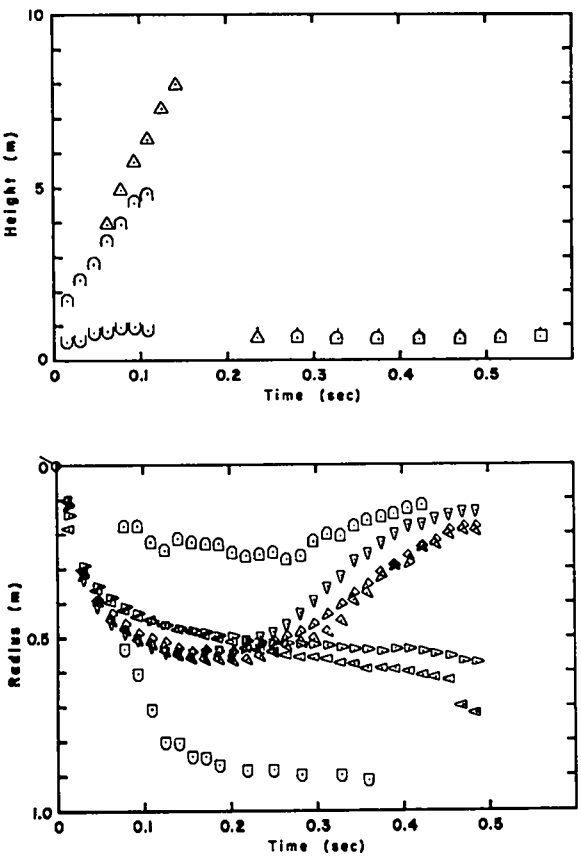

Fig. 7. Time history of Shot E-3689. The charge was 25.4 mm in diam, submerged 5/8 diam, and supported with thread so that the boom did not interfere and so that the MDF was inclined 60° from vertical. The average radius of the gas bubble was as large as, if not slightly larger, than that for any other shot with the same size charge. The symbols are defined in the caption of Fig. 3 with the addition of

$H_{R,P}$, height of remnant of stem - possibly combined with young plume

H_P, height of plume. The symbol shape is a stylized representation of the actual shape at the indicated time.

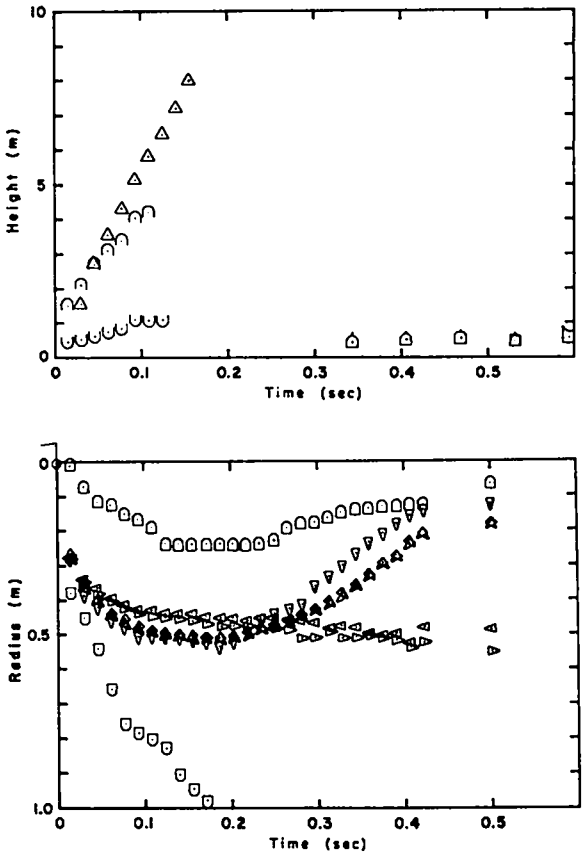

Fig. 8. Time history of Shot E-3681. The charge was 25.4 mm in diam, submerged 3/4 diam, supported so that the MDF was vertical and the support boom interfered with the water jet. Symbols are defined in the captions of Figs. 3 and 7 with appropriate stylized modifications to show the shape of stem remnants and plumes.

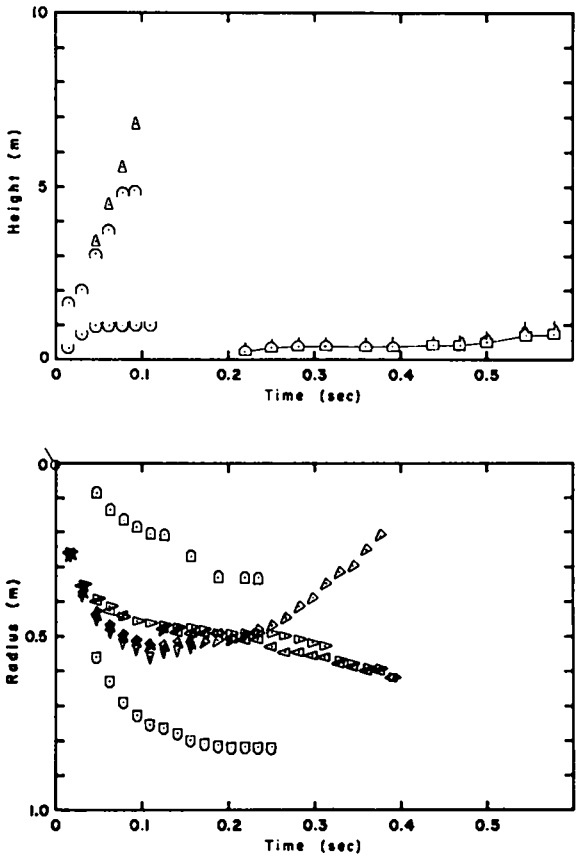

Fig. 9. Time history of Shot E-3686. This shot was a replicate of Shots E-3681 and E-3690 (Figs. 8 and 10) except for changes in the method of support and the angle of inclination of the MDF. The charge was partially supported by thread so that the MDF was inclined 30° from plumb and so that the support boom did not interfere with the water jet. Symbols are defined in the captions of Figs. 3 and 7 with appropriate stylized modifications to show the shape of the stem remnant and the plume.

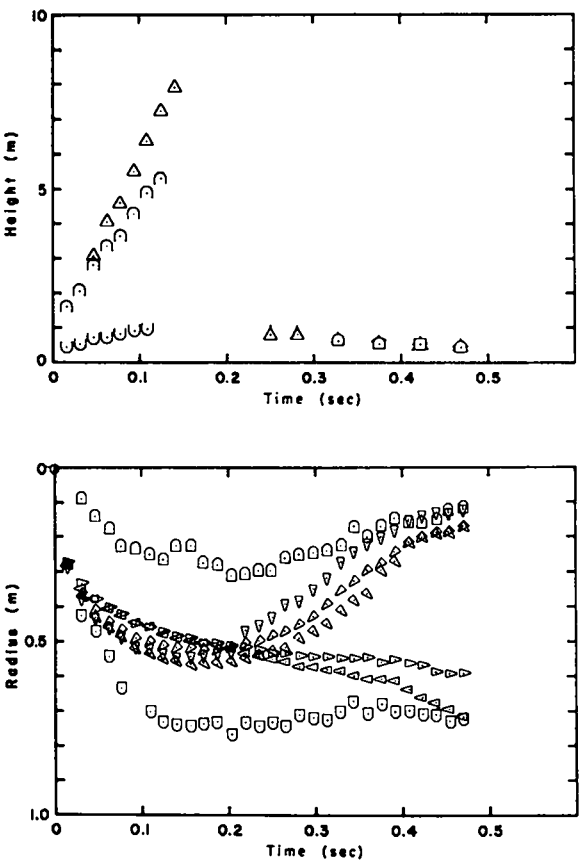

Fig. 10. Time history of Shot E-3690. This shot was a replicate of Shots E-3681 and E-3686 (Figs. 8 and 9) except the angle of inclination of the MDF was 75° from plumb. The support boom did not interfere with the water jet. Symbols are defined in the captions of Figs. 3 and 7. Comparison of Figs. 8 - 10 shows that variations in the support appear to affect the vertical growth of the root. However, the opposite effect on the growth rate caused by a given change in support was shown in Figs. 5 and 6.

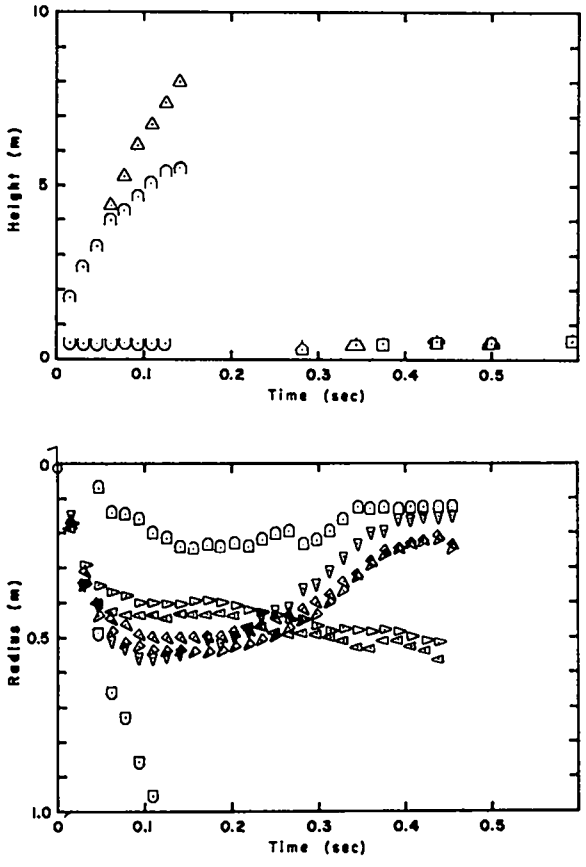

Fig. 11. Time history of Shot E-3682. The charge was 25.4 mm in diam, was just fully submerged, and was supported so that the MDF was vertical and so that the support boom interfered with the water jet.

Symbols are defined in captions of Figs. 3 and 7 with appropriate stylized modifications to show the shape of the stem remnant and the plume.

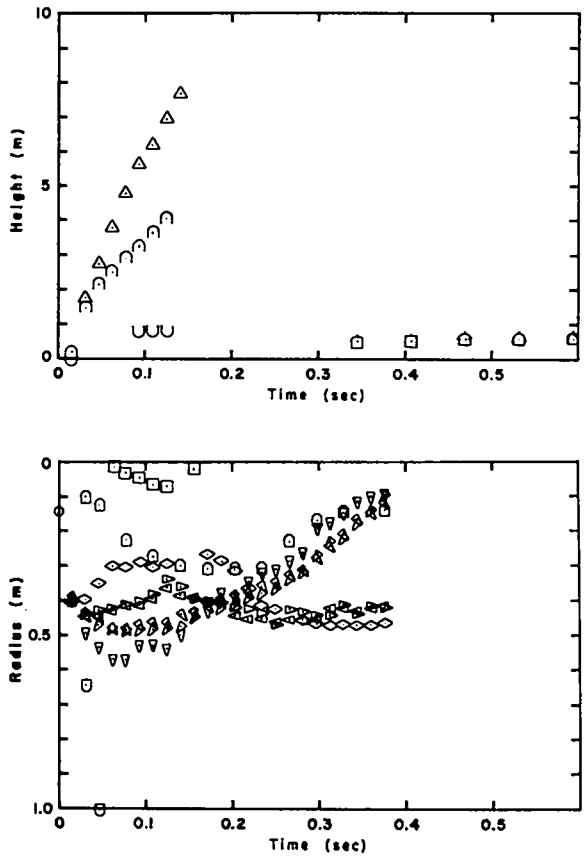

Fig. 12. Time history of Shot E-3683. The charge was 25.4 mm in diam and was submerged 6 diam. The MDF was vertical and the support boom interfered with the water jet. A long root with a very large diameter was observed in this shot. Consequently, the measurement of vertical radius of the gas bubble was exceptionally poor. Sub-surface details were significantly different.

Symbols are as for previous graphs except appropriate stylized modifications to show the shape of the stem remnant and the plume in the upper graph and as follows in the lower graph.

- ◇ $(R_{0-L} + R_{0-R}) \div 2$, i.e., average radius of the gas bubble or vent along the original water level.
- ◁ R_L, bubble radius to the left along a level through the charge center.
- ▷ R_R, bubble radius to the right along a level through the charge center.
- ⊡ H_V, vertical height of right circular vent.

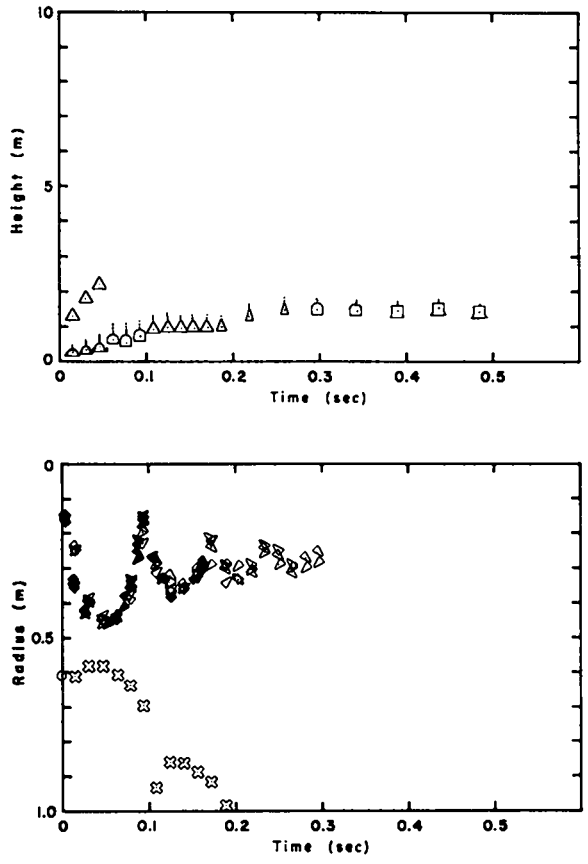

Fig. 13. Time history of Shot E-3691. The charge was 25.4 mm in diam and was submerged 24 diam. The MDF was vertical but the detonation cable was held well beyond the boom tip by thread so that the boom did not interfere with the water jet. The detonation products did not escape to form a gas cloud, the water jet was very small, and the stem or plume formation was unique. The gas bubble went through several oscillations, four of which are plotted. The center of the gas bubbles moved down with time until it vented to one side.

Upper Graph:

△ height of water jet.

△△△□ stylized symbols indicating height and shape of plume.

Lower Graph:

◁◁◁◁ radii along 45° lines through the point of symmetry of the gas bubble from synchronous motor camera record.

◀◀◀◀ bubble radii from Hycam camera (1666 f/sec) record.

✠ vertical coordinate of point of symmetry from synchronous motor camera record.

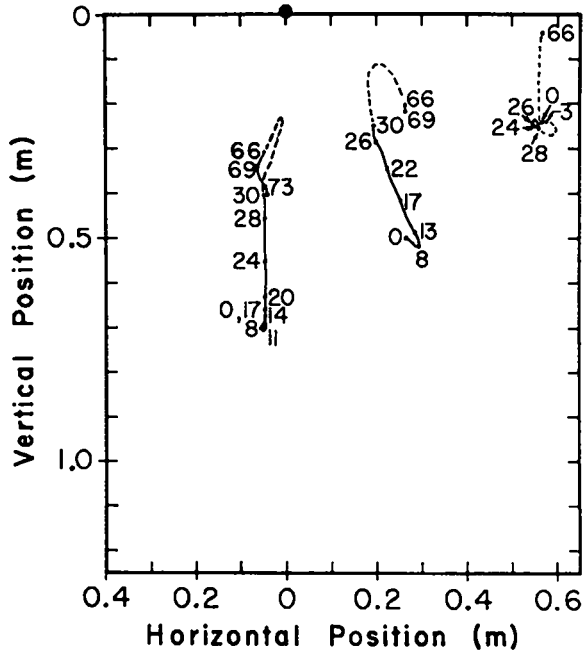

Fig. 14. Paths of mass markers (water-filled ping pong balls) from Shot E-3684. The charge was 25.4 mm in diam and was submerged 1/4 diam. The numbers near the various points are the frame numbers; the framing rate was 64 pictures/sec (pps). The origin is the intersection of the vertical center line through the charge with the water surface.

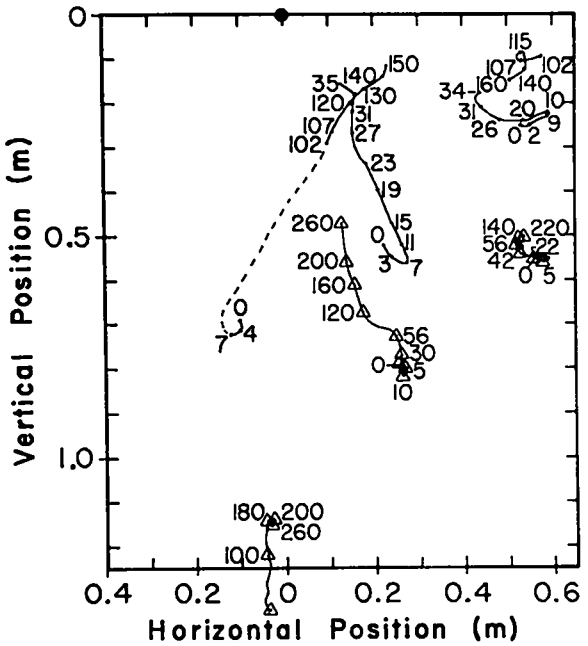

Fig. 15. Paths of mass markers for a 25.4-mm-diam charge submerged 1/2 diam. Shot E-3680 is represented by triangles and Shot E-3685 by dots. The numbers near the various points are the frame numbers at 64 pps beginning at the time of detonation. The origin is as in the previous graph.

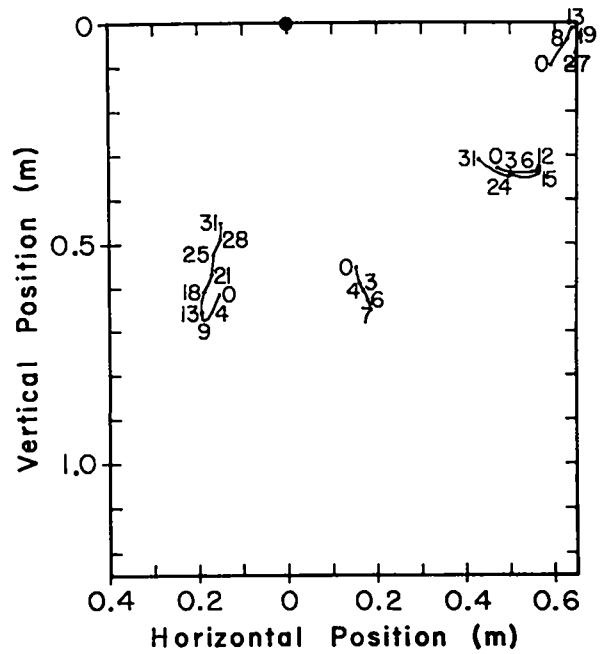

Fig. 16. Paths of mass markers from Shot E-3689. The charge was 25.4 mm in diam and was submerged 5/8 diam. The number near the various points are the frame numbers at 64 pps. The origin is as in the previous graphs.

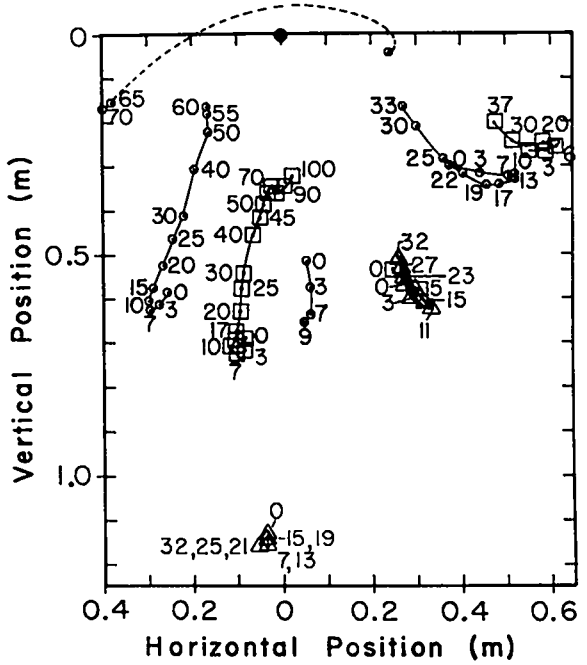

Fig. 17. Paths of mass markers from shots with 25.4-mm-diam charges submerged 3/4 diam. Triangles, squares, and circles represent Shots E-3681, E-3686, and E-3690, respectively. The numbers near the various points are the frame numbers as in previous graphs. The origin is as in the previous graphs.

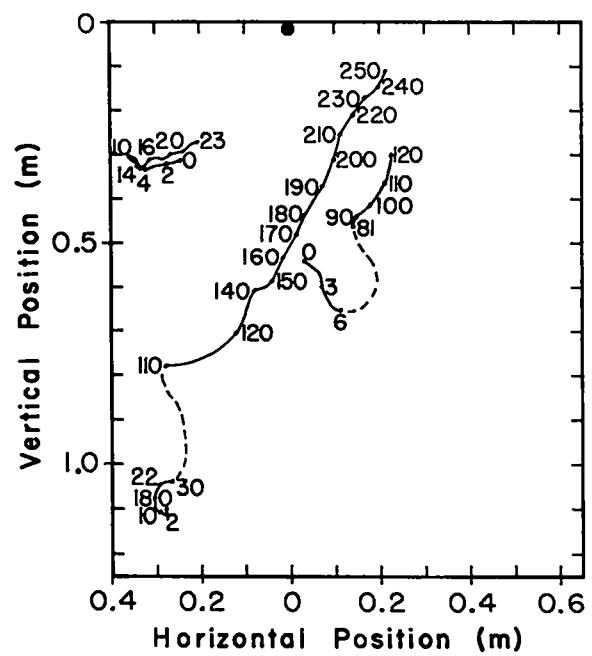

Fig. 18. Paths of mass markers for a 25.4-mm-diam charge just fully submerged (Shot E-3682). The numbers near the various points are the frame numbers as in previous graphs. The origin is as in previous graphs.

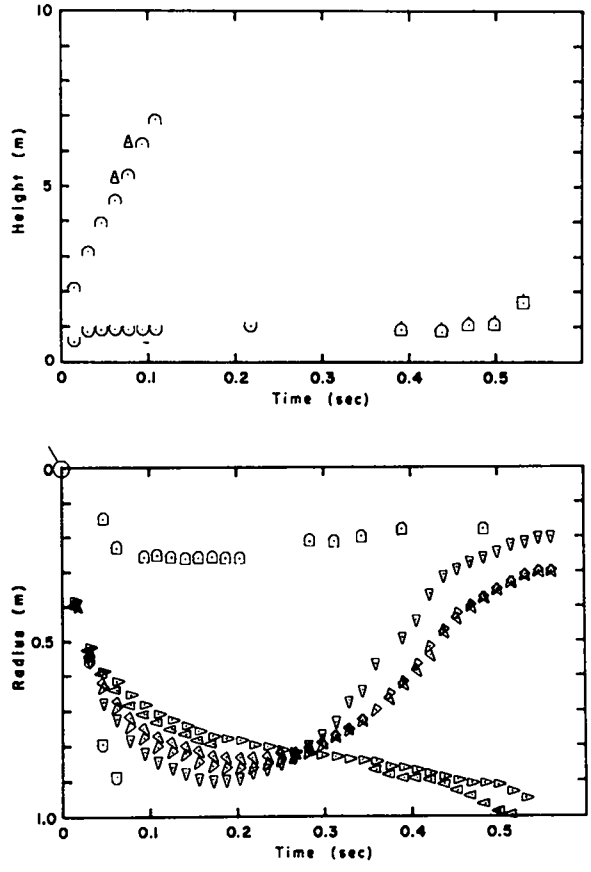

Fig. 19. Plot of early time data from the larger charge used in Shot E-3687. The charge was 50.8 mm in diam, submerged 1/2 diam, and supported by thread so that the MDF was inclined 30° from vertical. Although the tip of the support boom was well to one side, it did interfere, probably in a small way, with the large water jet.

Symbols carry the same meaning as in previous graphs of shots with the charge near the UCD.

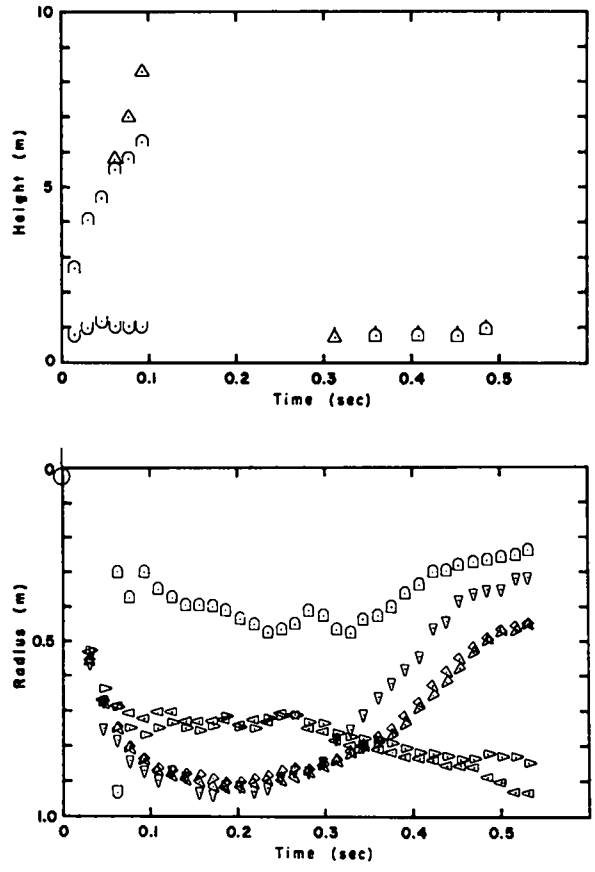

Fig. 20. Early time data from the larger charge just fully submerged (E-3692). The charge was 50.8 mm in diam, was just fully submerged, and was supported by thread so that the MDF was vertical but the boom tip was well to one side of the charge. Due to the large diameter of the water jet, the jet did strike the boom but was probably interfered with only trivially.

Origin and symbols the same meaning as in Figs. 14-18 for shots with the charge near the UCD.

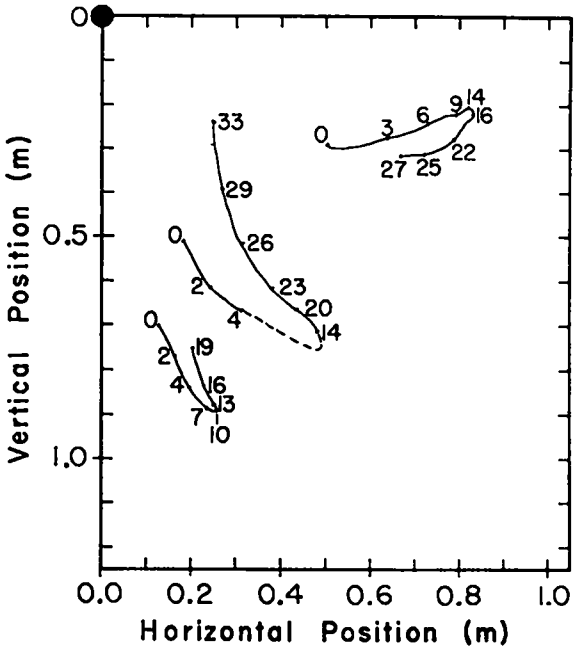

Fig. 21. Paths of mass markers for Shot E-3687; 50.8-mm-diam charge submerged 1/2 diam. The numbers near the various points are the frame numbers. The framing rate was 64 pps.

The origin is as described in the caption of Fig. 14.

25.4-mm-diam charges submerged 1/2 diam. Possibly the increased momentum associated with collapse of a larger bubble allowed penetration of the remnant. When the 50.8-mm-diam charge was just fully submerged the plume eruption was most apparent near the outside of the remnant of the stem as if the eruption was deflected by the remnant. The bubble diam at the surface was noticeably smaller when the charge was fully submerged than when submerged 1/2 diam. In both shots very large roots were produced.

Figure 22 shows tracings of the oscilloscope records obtained from the two conductivity gauges used in Shots E-3689 and E-3690. In Shot E-3689 one gauge was placed so that it would be engulfed by the gas bubble; the other gauge was placed so that it would not be engulfed. The closest gauge showed an abrupt decrease in conductivity, of a magnitude approximately the same as that found for air, at a time corresponding to the time when the gauge was engulfed by the gas bubble as measured from the framing camera photographs. The second gauge, located outside of the gas bubble, showed no change in conductivity. In Shot E-3690 one gauge was placed at about the same radius as that of the closest gauge in Shot E-3689; the second gauge was placed at a radius which would lead to engulfment at a later time. The conductivity of both gauges changed at times and in directions consistent with the framing camera photographs.

The motion pictures obtained in the early round of experiments suggested that a reasonably stable wave train was established within the tank. Accordingly a photographic arrangement for measuring wave amplitude as a function of time was added to the subsequent experiments.

Wave histories for two shots, measured at a range of about four meters from the detonation, are plotted as Fig. 23. In general, the first significant wave is of negative amplitude. It is speculated that this negative amplitude is a consequence

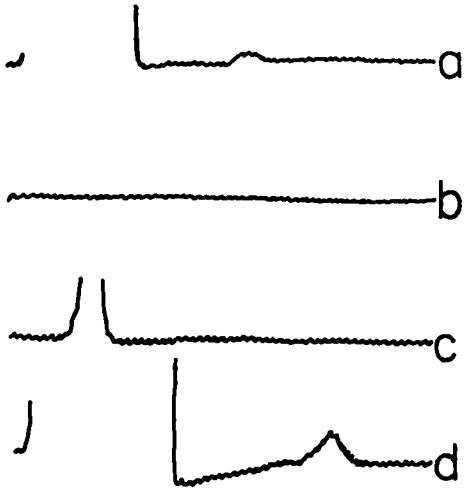

Fig. 22. Tracings of the oscilloscope records obtained with conductivity gauges. Time increases to the right.

a. Gauge closest to charge in Shot E-3689.

b. Gauge outside of gas bubble in Shot E-3689.

c. Gauge near extreme of bubble expansion in Shot E-3690.

d. Gauge closest to charge in Shot E-3690.

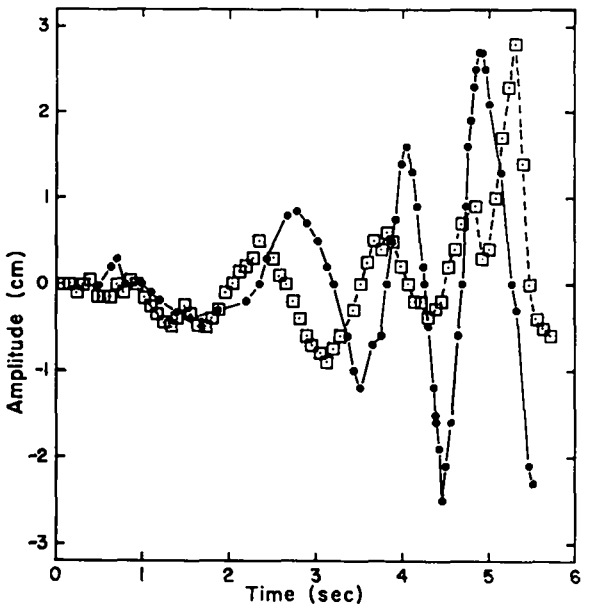

Fig. 23. Plot of wave amplitude during the first five seconds following explosion time for two 25.4-mm-diam charges. The solid circles are from Shot E-3689 in which the charge was submerged 5/8 diam and was the closest to the upper critical depth. The open squares are from Shot E-3691 in which the charge was submerged 24 diam and was the closest to the lower critical depth.

of water flow toward the cavity. The photographs suggest that this negative amplitude is well in front of the waves generated by the collapse of the plume.

It was also observed that the wave train from the detonation located closest to the upper critical depth was the most nearly sinusoidal at this range. There were no duplicate measurements of wave trains so it is not known if the apparent early organization from the detonation nearest the upper critical depth is accidental or real.

Measurements of the maximum wave amplitude are considered as only approximate because the gauge was located relatively close (0.69 m) to the side of the tank which might perturb the wave train by reflection. To minimize this probable source of error the maximum amplitude observed up to the time when the wave train broke over the edge of the tank (ca 20 mm above water level) was taken as the maximum amplitude of the train. This was not the largest amplitude observed but was nearly so.

The maximum amplitude as defined above has been scaled and plotted after the method of Pace et al.[8] in Fig. 24. It appears that the model of Pace et al. can be extrapolated to an order of magnitude smaller charge weight than those used for the model's calibration. It also appears that this work provides an independent confirmation of the upper critical depth phenomenon. The reasonable agreement with Pace et al. also lends support to claims that our tank approximated an infinite sea.

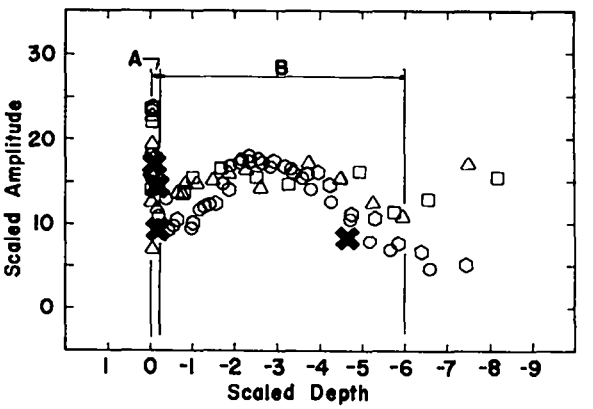

Fig. 24. Comparison of wave amplitudes as a function of charge depth as observed in my work with the observations of Pace et al. (taken from Fig. 3.8 of Ref. 8).
The solid crosses represent my work which had equivalent TNT charge weights of 0.017 and 0.136 kg. The open symbols represent the data of Pace et al. obtained with TNT charges; circles - 0.23 kg, hexagons - 0.91 kg, triangles - 56.8 kg, squares - 175 kg.

The scaled amplitude is $A_{max}R \div W^{0.60}$ for the upper critical depth region (the region A in the figure); the scaled amplitude is $A_{max}R \div W^{0.535}$ for the lower critical depth region (the region B). A_{max} is the maximum wave amplitude observed at range R; W is the TNT charge weight. The scaled depth is $Z \div W^{0.63}$ in the upper critical region and $Z \div W^{0.25}$ in the lower critical region. Z is the depth at which the center of the charge is submerged.

V. DISCUSSION

Although a significant amount of data has been presented, the reader should be aware that no collection of graphs and words can give as good a description of the phenomena as that contained in the camera photographs.

The observations of the pre-plume, water jet, and root in these experiments are especially significant because they were not anticipated. These features offer a possible explanation for how a maximum wave is generated by a detonation at the UCD.

When the detonation is above the UCD, as for Fig. 3, the pre-plume is small, the above-surface jet is mostly gas, the lip (radius at the surface) of the gas bubble is essentially as large as other radii, the root is small, and the representative gas bubble radii are not as large as when the detonation is at the UCD; consequently, the plume thrown up at collapse is of smaller diameter, does not have as large a volume, and is not given an outward component as when the plume is formed by a detonation at UCD.

At or near the UCD, as for Fig. 7, the representative radii of the gas bubble are largest, the pre-plume is large, the above surface jet contains a significant amount of water, the lip of the gas bubble offers only a little if any impediment to plume formation, and the root is large. Importantly, it appears that the water in the pre-plume and jet is such that the water thrown up at bubble collapse is deflected to give it a large outward component as well as upward component of motion. The outward and upward motion results in a very large splash wave early in the plume formation. It would not be surprising if other factors also contribute to the UCD phenomena.

When the detonation is a little below the UCD, as in Fig. 11, the lip of the representative radii for the gas bubble is smaller, the lip of the gas bubble confines or modifies formation of the plume, and the water jet and root are as large or larger than those for UCD. Also, it appears that the water in the pre-plume interacts differently with that thrown up when the gas bubble collapses. The resulting splash wave appears smaller and less organized than that for UCD.

With increasing depth the representative gas bubble radii, the oscillatory period, and the amount of venting decrease; the volume of the gas bubble may increase a little if the detonation is not too deep. Up to some depth, the water jet and the root appear to increase (Figs. 11 and 12); however, when the depth was sufficient so that only trivial early venting of the gas bubble occurred no root, and only a very small and weak water jet, were observed (Fig. 13). The plume resulting from a deep detonation is formed by an entirely different mechanism from that of a detonation near the UCD.

As shown in Fig. 13, the oscillating gas bubble had a general downward motion contrary to expectations from consideration of buoyancy alone; however, the observed motion is not in qualitative disagreement with the "image-source" model of Bryant.[3]

Comparisons of Fig. 5 with Fig. 6 and Fig. 8 with Fig. 9 or with Fig. 10 show that the growth of the gas bubbles is very reproducible; however, both above-surface phenomena and collapse of the gas bubbles are subject to considerable variation. At least part of the observed variations are due to variations in the charge support and in the inclination of the MDF.

Increasing the charge radius by a factor of two did not result in any clear qualitative change (Figs. 19 and 20). As expected, the gas bubble radii increased (ca 74%) for the larger charge submerged the same fraction of its diameter. The motion pictures do suggest that the collapse of the gas bubble in Shot E-3692 (Fig. 20), which had the charge just fully submerged, was favorable for producing a large splash wave.

A preliminary experiment which was performed in a smaller and differently shaped tank was discussed in LA-4958. A point of concern in the preliminary experiment was the cause of the root (called a stem in Reference 4) extending from the bottom of the gas bubble. It was hypothesized that the root might be due to either the small tank size, the method of support of the charge, or the MDF.

The tank greater than three times larger, variations in method of support, and variations in the angle of inclination of the MDF used in the current experiments all failed to eliminate the root. If the root is due only to the MDF one would expect

the root to be reduced by the use of a larger diameter charge; if anything, larger diameter charges produced larger roots. Furthermore, a root was not observed when the charge was deeply submerged (Fig. 13); the root was very small when the charge was shallow (Fig. 3). The water jet was also not observed when the charge was deeply submerged; the jet was very small and mostly gaseous when the charge was immersed less than the UCD. In short, there is a correlation between water jet and root.

The root does not seem to have been previously recognized as separate from the bubble, albeit an exhaustive search of the literature has not been made. Young and Hammond[5] cite Hendricks and Smith as observing an elongated bubble. Tracings of the bubble outline, as presented by Young and Hammond could be interpreted as an approximate hemispherical gas bubble plus a root. Young and Hammond did not use MDF to initiate their charges. A. R. Kriebel[6] also shows tracings which can be interpreted as hemispherical gas bubbles plus roots.* The gas bubbles in Kriebel's study were generated by exploding wires. Kriebel identifies the root in his experiments as a jet caused by inward collapse of the walls of the water column just before the cavity becomes fully expanded.

Pritchett[7] compared results of a sophisticated computer model with observations made of the WIGWAM event (nuclear explosion, 30 kt, 610 m below the surface of the Pacific Ocean in very deep water, May 14, 1955). Pritchett's model predicts a vortex below the collapsing and upward moving bubble. The author does not know if the WIGWAM event vented and jetted; however, it appears that Pritchett's vortex does not originate for the same reason that the root originates in UCD experiments.

The presence of the water jet, as such, also does not appear to have been previously recognized. Young and Hammond did comment ".....the radial flow model predicts a very thin water seal above the charge which travels at extremely high velocity long after intuition tells us that such a situation could prevail." It seems likely that the predicted in-flowing water seal is akin to the observed conical part of the inverted funnel shape described earlier. Convergence of this water would result in a jet.

*See Figs. 7 - 16 in Reference 6.

The water jet, being of relatively small diameter compared to other items of interest, is difficult to photograph, especially with black-and-white film against a sky background. Also, as happened in our preliminary experiment, the charge support can easily destroy or modify the water jet; this factor may also have contributed to previous failure to observe or recognize the water jet.

The maximum gas bubble radius along a line 45^{o} with respect to plumb was 47.7 cm in the preliminary experiment; this occurred at a time of about 0.19 sec. In the current experiments, with the same charge and submersion, values obtained for these parameters are 48 and 50 cm and 0.15 and 0.14 sec. In the current experiments the gas bubbles collapsed significantly faster than in the preliminary experiment with the small tank. These differences, although relatively small, suggest that the present tank is a reasonable approximation to an infinite sea for charges of 2.54-cm and 5.08-cm diam and a questionable approximation for 7.62-cm-diam charges.

The two-penny gauge results are interpreted as evidence that the bubble boundary as shown by photography is the boundary between detonation products and water. The results contradict speculation that the cameras might be recording a significant water cavitation or spall boundary rather than the products-water interface; estimates of the volume of water above surface and the volume of the gas cavity lend additional weight to contradict such speculation. A study of the photographic records and of Figs. 15 - 18 also shows that gauges must be either anchored solidly or photographed as a function of time if their position is important in the reduction of the data.

VI. SUMMARY

Data which partially describe the flow of water when a charge is detonated near the upper critical depth have been presented. The work appears to provide an independent confirmation of the upper critical depth phenomenon as well as to provide quantitative data useful for calibrating a computer model of the phenomena. In addition, a tentative qualitative description of the mechanism by which a charge detonated at the upper critical depth generates a maximum water wave has been proposed. This description involves the time at which the pre-plume and

water jet collapse relative to collapse time of the gas cavity as well as the size and shape of the cavity. The flow which produces the pre-plume, water jet, and root is not understood and therefore needs additional study.

ACKNOWLEDGMENTS

The author is grateful for the technical support of J. LaBerge, A. Gallegos, L. Stovall, and H. Langley of M-3 and B. Claybrook and R. Gordon of ISD-7. A. W. Campbell, J. R. Travis, W. C. Davis, B. Hayes - all of M-3, C. L. Mader of T-4, and K. Olsen of J-9 provided technical support. B. D. Lambourn of A.W.R.E. called my attention to Reference 3.

This work was performed for the U. S. Atomic Energy Commission Tamarin Committee.

REFERENCES

1. Bernard LeMehaute, "Theory of Explosion-Generated Water Waves," Advan. in Hydrosci. 7, 1 (1971).
2. Charles L. Mader, LA-4958, "Detonation Near the Water Surface," June 1972.
3. A. R. Bryant, "The Gas Globe," Underwater Explosion Research 2 (Published by ONR) (1950).
4. J. W. Hendricks and D. L. Smith, "Above and Below Surface Effects of One-Pound Underwater Explosion." Hydra I. (US) NRDL-TR-480 (1960).
5. F. H. Young and R. R. Hammond, "A Non-Spherical Model Describing the Motion of a Shallow Underwater Explosion Bubble." (US) NRDL-TR-771 (1964).
6. A. R. Kriebel, "Simulation of Underwater Nuclear Bursts at Shallow Depths with Exploding Wires." URS7028-1 (1971).
7. J. W. Pritchett, Second International Conference on Numerical Methods in Fluid Dynamics (Berkeley, California, Sept. 1970).
8. C. E. Pace, et al, "Effect of Charge Depth of Submergence on Wave Height and Energy Coupling," WES-TR-1-647-4.